Detection of damage in concrete using diffuse ultrasound (L)

Frederik Deroo and Jin-Yeon Kim
School of Civil and Environmental Engineering, Georgia Institute of Technology, Atlanta, Georgia 30332-0355

Jianmin Qu and Karim Sabra
G. W. Woodruff School of Mechanical Engineering, Georgia Institute of Technology, Atlanta, Georgia 30332-0405

Laurence J. Jacobs
School of Civil and Environmental Engineering and G. W. Woodruff School of Mechanical Engineering, Georgia Institute of Technology, Atlanta, Georgia 30332-0360

(Received 9 September 2009; revised 23 March 2010; accepted 31 March 2010)

This letter demonstrates the potential for using diffuse ultrasound measurements to detect damage in concrete. Two different solutions to the diffusion equation, an infinite three-dimensional (3D) volume model that neglects geometric boundaries and a finite 3D cuboid model, are used for the required curve fitting procedure to determine the influence of geometric boundaries on the solution. The measurements consider two types of microcrack damage in concrete, alkali-silica reaction and thermal damage, and show that the measured diffusivity parameter is related to the amount of damage in each specimen. © *2010 Acoustical Society of America.* [DOI: 10.1121/1.3409480]

PACS number(s): 43.35.Cg, 43.20.Gp [JAT] Pages: 3315–3318

I. INTRODUCTION

Concrete is a multiphase, heterogeneous, multiple length scale material consisting of a cement-paste matrix plus fine (sand) and coarse (gravel) aggregates. The heterogeneities in concrete such as the random distribution of aggregate in the cement-paste matrix lead to strong scattering of ultrasonic waves at wavelengths on the order of the aggregate. Use of relatively high ultrasonic frequencies—typically in the high kHz to low MHz range—is necessary to detect damage at an early stage. The ultrasound energy density in this regime can be described by the diffusion equation. This research develops a quantitative understanding of the effects of additional scattering sources, such as microcracks in the cement-paste matrix due to alkali-silica reaction (ASR), on the diffusion and the dissipation coefficients. Two different solutions of the diffusion equation are used for the required curve fitting procedure—a three-dimensional (3D) infinite volume model neglecting geometric boundaries and a finite 3D cuboid model.

Previous research used diffuse ultrasound to investigate randomly distributed glass spheres immersed in water[1] and the microstructure of aluminum foam and polycrystals.[2,3] Anugonda *et al.*[4] applied diffuse ultrasound to concrete and determined the diffusion parameters, while Ramamoorthy *et al.*[5] determined the depth of surface breaking cracks in concrete specimens with diffuse ultrasound. Becker *et al.*[6] examined the effect of microstructure on the diffuse ultrasound field and show that the dissipation coefficient is directly related to the amount of viscoelastic cement-paste matrix in a specimen.

The objective of this research is to detect microcrack damage in concrete by determining the diffusivity and dissipation with two different diffusion equation solutions, and then comparing them for specimens with different damage levels.

II. ULTRASONIC DIFFUSION APPROXIMATION

The diffuse method is based on the assumption that the spectral energy density of an ultrasonic wave field can be described by the diffusion equation, after the wave field has been strongly scattered. This diffuse field is spatially and temporarily incoherent with the incident signal and the field variables are considered to be random. The diffusion equation that describes the time evolution of the spectral energy density $\langle E(\vec{x},t,f)\rangle$ (energy per frequency, per volume) of an ultrasonic wave field is given by

$$\frac{\partial\langle E(\vec{x},t,f)\rangle}{\partial t} - D\Delta\langle E(\vec{x},t,f)\rangle + \sigma\langle E(\vec{x},t,f)\rangle = P(\vec{x},t,f)\ \forall\ \vec{x}\in\mathcal{B}. \quad (1)$$

$P(\vec{x},t,f)$ is the spectral source energy density (forcing condition), D is the frequency-dependent diffusion coefficient, and σ is the dissipation rate.[2] The body is assumed to be isotropic, so the diffusion coefficient does not depend on direction. $\langle\cdot\rangle$ represents the expected value operator, i.e., Eq. (1) describes the evolution of the ensemble average energy density. $\mathcal{B}$ describes the elastic body considered and Δ is the Laplacian. Rapid spatial fluctuations in phase and amplitude cause the diffuse field to converge to zero if it is averaged over random configurations or spatially averaged; this effect is called phase cancellation. It is important to note that no energy is lost in scattering, so scattering does not contribute to σ. Also, note that the diffusivity D depends on the material microstructure; higher D means faster diffusion of the energy through the material, so it is expected that increased scatter-

ing due to damage slows down the diffusion, which results in lower D values.

This research considers two solutions of the diffusion equation to curve fit experimentally measured spectral energy density curves to recover the two parameters of interest, diffusivity D, and dissipation σ.

The first solution is a 3D, infinite body. The solution is given by[7]

$$\langle E(x,y,z,t)\rangle = \frac{P_0}{8(D\pi t)^{3/2}} e^{-(x^2+y^2+z^2)/4Dt} e^{-\sigma t}, \quad (2)$$

where P_0 is the magnitude of the source pulse. An advantage of this infinite solution is that an easy linear regression to the measured data is possible after taking the natural logarithm of both sides. Note that assuming that the specimen is infinite will not necessarily be accurate in this application, since the specimen has finite dimensions with boundaries. However, this infinite model is attractive because: of its simplicity; that it can be used as a first pass to estimate the trends in diffusivity and dissipation; and the values determined here can serve as an initial guess for the more complex nonlinear curve fitting procedure needed for the finite 3D model.

The second solution is a finite 3D model of a cuboid with dimensions $a\times b\times c$ with an impulse excitation at the point (x_0,y_0,z_0) which yields $P(x,y,z,0)=P_0\delta(t)\delta(x-x_0)\delta(y-y_0)\delta(z-z_0)$. The high impedance mismatch between the concrete and the surrounding air leads to the assumption that there is no ultrasonic flux in the outward direction of the specimen. The finite 3D solution is derived using Fourier series[5,8] and is given by

$$\begin{aligned}\langle E(x,y,z,t)\rangle = P_0 e^{-\sigma t}\{&1 + [g(x,x_0;a)g(y,y_0;b)g(z,z_0;c)] \\ &+ [g(x,x_0;a) + g(y,y_0;b) + g(z,z_0;c)] \\ &+ [g(x,x_0;a)g(y,y_0;b) \\ &+ g(x,x_0;a)g(z,z_0;c) \\ &+ g(y,y_0;b)g(z,z_0;c)]\}, \end{aligned} \quad (3)$$

where

$$g(X,X_0;A) = 2\sum_{n=1}^{\infty} \cos\left(\frac{n\pi X}{A}\right)\cos\left(\frac{n\pi X_0}{A}\right) e^{-D(n\pi/A)^2 t}, \quad (4)$$

(x,y,z) is the receiver position and (x_0,y_0,z_0) is the source position.

III. EXPERIMENTAL PROCEDURE

The concrete specimens used in this research have the dimensions $75\times75\times46$ mm^3 and are cut from bars 285 mm long that are cast according to ASTM C 1293,[9] a standard test to quantify the reactivity of an aggregate to ASR. ASR is the chemical reaction of alkalis from the cement, with silicas from the aggregate, which form an alkali-silica gel. This gel has the propensity to absorb large quantities of water and swell, which causes expansion, and eventually microcracking of the concrete.[10] Expansion tests following ASTM C 1293 track this change in length over time (in this case a total of 2 years) to characterize the overall ASR damage level in each specimen. This research considers three specimens with different levels of ASR damage: specimen ASR1 (most damage with an expansion of 0.46%); ASR6 (medium damage with an expansion of 0.30%); and ASR7 (least damage with an expansion of 0.08%). Note that all three of these expansions are relatively large; even specimen ASR7 just exceeds the "acceptable" level of ASTM C 1293. Note that while there is a potential correlation between the expansion and the ASR damage state, the expansion does not necessarily indicate the level of damage in a quantitative manner. However these expansion results have been established as an independent measure of the likelihood of the overall ASR damage level in each specimen.[11,12] The thermal damage specimen starts with an ASR damaged specimen (ASR6) and subjects it to heat at 120 °C. This heat is cyclically applied in 3 h intervals for a 9 h total; between every 3 h interval, the specimen cools down to room temperature for the diffuse measurements. This heating causes the free water in the concrete to evaporate, which leads to an expansion and additional microcracking in the material.[13]

A high-voltage pulse generator provides the 400 V source signal, and two 1 MHz broadband transducers are used as the source and receiver. An aluminum cone (bottom diameter 5 mm, top diameter 2 mm, and thickness 2.2 mm) is glued to the surface of the receiving transducer to reduce the surface area, a requirement to avoid phase cancellation. A fixture is designed and manufactured to keep the otherwise unstable transducer perfectly perpendicular to the surface. The impulse responses of different specimens are measured 38 mm off of the epicenter on the opposite side with respect to the source; the z-coordinates of the source (z_0) and receiver (z) are 46 mm and 0, respectively. The source transducer is set in the center, and the receiver close to the corner. In that configuration, when the receiver is placed near a corner, the maximum number of receiving points with the same source/receiver distance (i.e., points on a circle with radius r) are available on a specimen. It can be seen in Eq. (2) that points with equal source/receiver separation in an infinite volume should theoretically have the same expected value for the spectral energy density $\langle E\rangle$, which is in general not true for this measurement configuration since the distance to the boundaries change as the polar angle is varied. However, these differences should not dominate and are likely smaller than the scatter in the data. The same is true for the finite 3D model, where placing the receiver in a different corner corresponds to a rotation of the coordinate system, so that the coordinates (x,y,z) and (x_0,y_0,z_0) stay the same for every configuration with the same source/receiver distance. All measurements are filtered with a 4 MHz low pass filter, amplified, sampled with a sampling frequency f_s of 50 MHz, recorded with 200 000 record points and then 500 time signals are averaged to obtain the time-domain signal to be processed.

IV. EXPERIMENTAL RESULTS AND DISCUSSION

The signal processing procedure to obtain the spectral energy density from a measured ultrasonic time-domain signal is: windowed with a window length Δt with a specific window overlap; the discrete-time Fourier transform of the

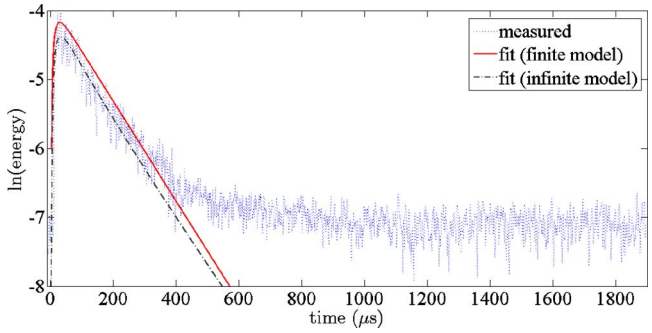

FIG. 1. (Color online) Spectral energy density with corresponding curve fits (f_c=350 kHz).

time window is taken and squared; the spectral energy density of each time window in a certain frequency bandwidth is determined by integrating the power spectrum in that bandwidth with width Δf centered around frequency f_c. Note the resulting quantity differs from $\langle E \rangle$ by an unknown constant related to the transducer sensitivity.[3] The values used for this research are Δf=350 kHz, Δt=6 μs, and window overlap of 90% between consecutive windows. For the infinite solution, a simple linear regression is used to determine the parameters D and σ. The finite solution requires a more complicated nonlinear curve fitting procedure; for example, this study uses a standard MATLAB function, lsqnonlin. Figure 1 shows typical data for the spectral energy density for both the infinite and finite 3D models.

First, consider the infinite solution, where the extracted parameters D and σ for the three ASR damaged specimens are shown in Fig. 2. These values are determined by averaging parameters from 10–14 separate measurements per specimen to achieve a better representation. The error bars correspond to the standard deviation. The diffusivity D shows a clear trend of lower magnitude for the more damaged specimens, while the dissipations for all three damage levels are almost identical; this is in good agreement with what is physically expected. The diffusivity curves get closer together at higher frequencies, most likely due to higher measurement uncertainty associated with the lower signal-to-noise ratio and fewer usable data points. The extracted parameters for the thermal damaged specimen are shown in Fig. 3, where the increase in microcracking due to increased heating times clearly results in a decrease in diffusivity, D. Note that the largest decrease in D occurs during the first heating cycle, so most of the additional damage most likely

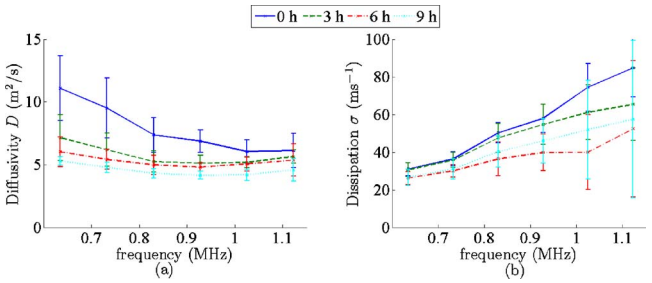

FIG. 3. (Color online) Diffusivity D and dissipation σ for thermal damaged specimens with infinite 3D model.

occurs during this first heating cycle. Overall, there is not expected to be a direct, one-to-one relationship between the change in diffusivity, D and expansion; ASR damage is a complicated process and will most likely require a predictive, physics-based model to quantitatively connect the ultrasonic measurements with damage. Finally note that there is no clear pattern in dissipation, σ.

Next, the finite 3D solutions for the ASR damaged specimens are shown in Fig. 4, each of which represents the average of 8–10 measurements. The trend is similar to that seen in the infinite solution, where the diffusivity D decreases with increasing damage, while the dissipation remains almost unchanged. The thermal damage results from the finite 3D model shown in Fig. 5 are similar to those of the infinite 3D model. Overall the error bars for the finite solutions are larger than those for the infinite solutions. These larger variations probably stem from the significantly larger complexity of the model (and the associated uncertainties) and the more complicated nonlinear curve fitting method required for the finite solution. However, the absolute values of D calculated from both the infinite and finite models are in the same range. Finally note that previous research[12] used nonlinear ultrasound to distinguish the amount of ASR damage in a variety of mortar samples; these complementary nonlinear ultrasonic measurements strengthen the validity of these diffusive ultrasound measurement results.

V. CONCLUSION

These results demonstrate the potential for using diffuse ultrasound to quantify microcrack damage in concrete in a reliable fashion. Both of the recovered parameters show the expected behavior: the diffusivity D decreases with increasing microcrack damage, while the dissipation σ has minimal

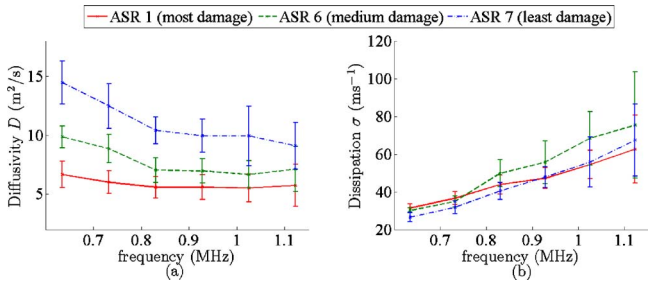

FIG. 2. (Color online) Diffusivity D and dissipation σ for ASR damaged specimens with infinite 3D model.

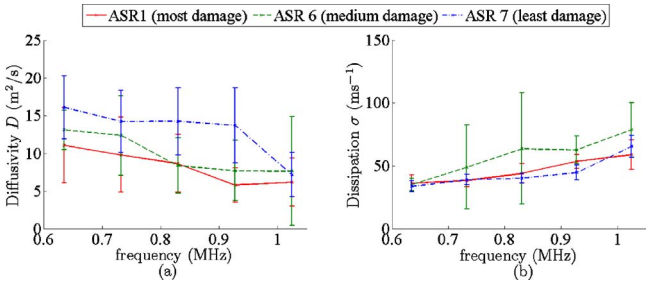

FIG. 4. (Color online) Diffusivity D and dissipation σ for ASR damaged specimens with 3D finite cuboid model).

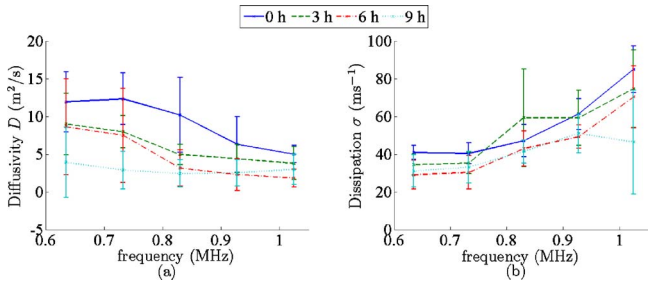

FIG. 5. (Color online) Diffusivity D and dissipation σ for thermal damaged specimens with 3D finite cuboid model.

changes. This decrease in diffusivity is due to the increased scattering from the microcracks, which slows down the diffusion process, while the intrinsic absorption is not significantly influenced by the microcracks. The infinite and finite 3D models show identical qualitative trends, even though the simpler infinite model shows higher robustness, presumably due to its simplicity.

ACKNOWLEDGMENTS

The Deutscher Akademischer Austauschdienst (DAAD) provided partial support to F.D.

[1]J. H. Page, H. P. Schriemer, A. E. Bailey, and D. A. Weitz, "Experimental test of the diffusion approximation for multiply scattered sound," Phys. Rev. E **52**, 3106–3114 (1995).
[2]R. L. Weaver, "Diffusivity of ultrasound in polycrystals," J. Mech. Phys. Solids **38**, 55–86 (1990).
[3]R. L. Weaver, "Ultrasonics in an aluminum foam," Ultrasonics **36**, 435–442 (1998).
[4]P. Anugonda, J. S. Wiehn, and J. A. Turner, "Diffusion of ultrasound in concrete," Ultrasonics **39**, 429–435 (2001).
[5]S. K. Ramamoorthy, Y. Kane, and J. A. Turner, "Ultrasound diffusion for crack depth determination in concrete," J. Acoust. Soc. Am. **115**, 523–529 (2004).
[6]J. Becker, L. J. Jacobs, and J. Qu, "Characterization of cement-based materials using diffuse ultrasound," J. Eng. Mech. **129**, 1478–1484 (2003).
[7]H. S. Carslaw and J. C. Jaeger, *Conduction of Heat in Solids* (Clarendon, Oxford, 1990).
[8]J. M. Hill and J. N. Dewynne, *Heat Conduction* (Blackwell Scientific, Boston, MA, 1987).
[9]ASTM-International, Standard test method for determination of length change of concrete due to alkali-silica reaction c 1293 08b (2008).
[10]K. E. Kurtis and P. J. M. Monteiro, "Chemical additives to control expansion of alkali-silica reaction gel: Proposed mechanisms of control," J. Mater. Sci. **38**, 2027–2036 (2003).
[11]M. B. Haha, E. Gallucci, A. Guidoum, and K. L. Scrivener, "Relation of expansion due to alkali silica reaction to the degree of reaction measured by SEM image analysis," Cem. Concr. Res. **37**, 1206–1214 (2007).
[12]J. Chen, J. Jayapalan, K. E. Kurtis, J.-Y. Kim, and L. J. Jacobs, "Nonlinear wave modulation spectroscopy method for ultra-accelerated assessment of alkali-silica reaction in Portland cement mortar," ACI Mater. J. **106**, 340–348 (2009).
[13]C. Payan, V. Garnier, J. Moysan, and P. A. Johnson, "Applying nonlinear resonant ultrasound spectroscopy to improving thermal damage assessment in concrete," J. Acoust. Soc. Am. **121**, EL125–EL130 (2007).